Separation Science and Technology

Publication details, including instructions for authors and subscription information:
http://www.informaworld.com/smpp/title~content=t713708471

Photochemical Behavior of the Insecticide Methomyl Under Different Conditions

Andjelka Tomašević[a]; Dušan Mijin[b]; Ernő Kiss[c]
[a] Institute of Pesticides and Environmental Protection, Belgrade-Zemun, Serbia [b] University of Belgrade, Faculty of Technology and Metallurgy, Belgrade, Serbia [c] University of Novi Sad, Faculty of Technology, Bulevar Cara Lazara, Novi Sad, Serbia

To cite this Article Tomašević, Andjelka , Mijin, Dušan and Kiss, Ernő(2010) 'Photochemical Behavior of the Insecticide Methomyl Under Different Conditions', Separation Science and Technology, 45: 11, 1617 — 1627
To link to this Article: DOI: 10.1080/01496395.2010.487720
URL: http://dx.doi.org/10.1080/01496395.2010.487720

Separation Science and Technology, 45: 1617–1627, 2010
Copyright © Taylor & Francis Group, LLC
ISSN: 0149-6395 print/1520-5754 online
DOI: 10.1080/01496395.2010.487720

Photochemical Behavior of the Insecticide Methomyl Under Different Conditions

Andjelka Tomašević,[1] Dušan Mijin,[2] and Ernő Kiss[3]
[1]*Institute of Pesticides and Environmental Protection, Belgrade-Zemun, Serbia*
[2]*University of Belgrade, Faculty of Technology and Metallurgy, Belgrade, Serbia*
[3]*University of Novi Sad, Faculty of Technology, Bulevar Cara Lazara, Novi Sad, Serbia*

This article describes the photolytic and photocatalytic removal of the insecticide methomyl at low concentration from different types of water, upon UV, visible or natural solar light radiation, in the presence of TiO_2 and ZnO, as well as using Fe-ZSM-5 zeolite and AlFe-pillared montmorillonite (photo-Fenton process). The rate of photodecomposition of methomyl was measured using UV spectrometry and HPLC, while its mineralization was investigated by ion chromatography (IC) and total organic carbon (TOC) analysis. The photochemical removal of methomyl is a natural and applicable model for the purification of water.

Keywords heterogeneous iron catalysts; methomyl; photocatalysis; photolysis; titanium dioxide; zinc oxide

INTRODUCTION

Methomyl (Fig. 1), with the IUPAC name *S*-methyl *N*-(methylcarbamoyloxy)thioacetimidate and CAS No. 16752-77-5 belongs to a class of compounds known as oxime carbamates (or carbamoyloxime). It was widely used for the control of insect and nematode pests. It is a very toxic and hazardous compound and a pollutant causing environmental concern because of its high solubility in water (57.9 g L^{-1} at 25°C), according to (1). Like some other closely related carbamates, methomyl acts by inhibiting the enzyme acetylcholinesterase (2). Since its sorption affinity to soils is rather low, it can easily cause contamination of both ground and surface water resources (3).

Advanced Oxidation Processes (AOPs) include catalytic and photochemical methods which use H_2O_2, O_3, or O_2 as the oxidant. The principal active species in these systems is the hydroxyl radical $^{\cdot}OH$, which is an extremely reactive and non-selective oxidant for organic contaminants (4,5). The main advantage of these processes is a complete mineralization of many organic pollutants (6,7). Several catalysts have been used (TiO_2, ZnO, Fe_2O_3, CdS, ZnS) and among them TiO_2 is one of the most effective (8–11). The following mechanism has been proposed:

a) absorption of efficient photons by titania ($h\nu \geq E_g = 3.2\,\mathrm{eV}$);

$$\mathrm{TiO_2} + h\nu(\mathrm{UV}) \rightarrow \mathrm{e^-_{CB}} + \mathrm{h^+_{\nu B}} \qquad (1)$$

b) oxygen ionosorption;

$$(\mathrm{O_2})_{\mathrm{ads}} + \mathrm{e^-_{CB}} \rightarrow \mathrm{O_2^{\cdot-}} \qquad (2)$$

c) neutralization of OH^- groups into $^{\cdot}OH$ radicals by photoholes;

$$(\mathrm{H_2O} \leftrightarrow \mathrm{H^+} + \mathrm{OH^-})_{\mathrm{ads}} + \mathrm{h^+_{\nu B}} \rightarrow \mathrm{H^+} + {}^{\cdot}\mathrm{OH} \qquad (3)$$

d) oxidation of the organic reactant via successive attacks by $^{\cdot}OH$ radicals;

$$\mathrm{R} + {}^{\cdot}\mathrm{OH} \rightarrow \mathrm{R'^{\cdot}} + \mathrm{H_2O} \qquad (4)$$

e) or by direct reaction with holes;

$$\mathrm{R} + \mathrm{h^+} \rightarrow \mathrm{R^{\cdot+}} \rightarrow \text{degradation products} \qquad (5)$$

As an example of the last process, the holes can generate CO_2 according to:

$$\mathrm{RCOO^-} + \mathrm{h^+} \rightarrow \mathrm{R^{\cdot}} + \mathrm{CO_2} \qquad (6)$$

ZnO is also frequently used as a catalyst in heterogeneous photocatalytic reactions. The biggest advantage of ZnO in comparison to TiO_2 is that it absorbs over a larger fraction of the UV spectrum and the corresponding threshold wavelength of ZnO is 387 nm. Upon irradiation, valence band electrons are promoted to the conduction band leaving a positive hole behind. These electron–hole

---

Received 12 December 2009; accepted 2 February 2010.

Address correspondence to Andjelka Tomašević, Institute of Pesticides and Environmental Protection, Banatska 31b, Belgrade-Zemun 11080, Serbia. Tel.: ++381(11)3076 133; Fax: ++381(11)3076 136. E-mail: academia@beotel.net

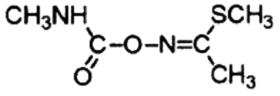

FIG. 1. Structure of methomyl.

pairs can either recombine or interact separately with other molecules. The holes in the valence band at the ZnO surface can oxidize adsorbed water or hydroxide ions to produce hydroxyl radicals. Electron in the conduction band at the catalyst surface can reduce molecular oxygen to superoxide anions. These radicals may form organic peroxides or hydrogen peroxide in the presence of organic scavengers. The hydroxyl radicals attack organic compounds (R) and intermediates (Int) are formed. These intermediates react with hydroxyl radicals to produce the final products (P). The mechanism of heterogeneous photocatalysis in the presence of ZnO can be given by the following reactions (12,13):

$$\mathrm{ZnO} + h\nu(\mathrm{UV}) \rightarrow \mathrm{e}^-_{\mathrm{CB}} + \mathrm{h}^+_{\mathrm{VB}} \tag{7}$$

$$\mathrm{e}^-_{\mathrm{CB}} + \mathrm{h}^+_{\mathrm{VB}} \rightarrow \mathrm{heat} \tag{8}$$

$$\mathrm{h}^+_{\mathrm{VB}} + \mathrm{H_2O_{ads}} \rightarrow \mathrm{H}^+ + {}^{\bullet}\mathrm{OH_{ads}} \tag{9}$$

$$\mathrm{h}^+_{\mathrm{VB}} + {}^-\mathrm{OH_{ads}} \rightarrow {}^{\bullet}\mathrm{OH_{ads}} \tag{10}$$

$$\mathrm{e}^-_{\mathrm{CB}} + \mathrm{O_2} \rightarrow \mathrm{O}_2^{\bullet -} \tag{11}$$

$$\mathrm{O}_2^{\bullet -} + \mathrm{HO}^{\bullet}_2 + \mathrm{H}^+ \rightarrow \mathrm{H_2O_2} + \mathrm{O_2} \tag{12}$$

$$\mathrm{O}_2^{\bullet -} + \mathrm{R} \rightarrow \mathrm{R{-}OO}^{\bullet} \tag{13}$$

$${}^{\bullet}\mathrm{OH_{ads}} + \mathrm{R} \rightarrow \mathrm{Int.} \rightarrow \mathrm{P} \tag{14}$$

Fenton's processes belong to AOPs that utilize H_2O_2 activation by iron salts. The classic Fenton's reagent is a mixture of ferrous ions and H_2O_2 in acidic solution or suspension (7,14):

$$\mathrm{Fe}^{2+} + \mathrm{H_2O_2} \rightarrow \mathrm{Fe}^{3+} + \mathrm{OH}^- + {}^{\bullet}\mathrm{OH} \tag{15}$$

Equation (15) presents the most important steps of a Fenton reaction and involves electron transfer between H_2O_2 and Fe(II) with the oxidation of Fe(II) to Fe(III) and the resulting production of highly reactive hydroxyl radicals $^{\bullet}OH$ and potentially reactive ferryl species. The removal of organic compounds by Fenton's reagent can be strongly accelerated by irradiation with UV or UV-visible light. This process is called the photo-Fenton reaction (14–17). Equation (15) is the key of photo-Fenton processes. The obtained Fe^{3+} ions or their complexes subsequently act as light absorbing species, which produce another hydroxyl radical, while the initial Fe^{2+} ion is regained:

$$\mathrm{Fe(OH)}^{2+} + \mathrm{hv} \rightarrow \mathrm{Fe}^{2+} + {}^{\bullet}\mathrm{OH} \tag{16}$$

The main advantage of the photo-Fenton process is light sensitivity up to a wavelength of 600 nm (17). According to the literature (5), irradiation with light of wavelength $\lambda < 580\,\mathrm{nm}$ affects the photoreduction of Fe^{3+} to Fe^{2+} together with the production of $^{\bullet}OH$ radicals.

The photolysis of different pesticides was frequently studied (18–20) but, to the best of our knowledge, there are no reported studies focusing on the photolysis of methomyl in the any type of water, including seawater. On the contrary, methomyl was successfully photodegraded using AOPs. Different catalysts were used, mostly TiO_2 (16,21–26). ZnO was also used (23). The photo-Fenton reaction was also employed (14,16,24–26), with dissolved ferrous sulfate heptahydrate being used as the source of Fe^{2+} ions. Recently, it was reported as a letter that methomyl can be photocatalytically removed using supported iron catalysts such as Fe-ZSM-5 zeolite and AlFe-pillared montmorillonite (27).

The objective of the present work was to study the photolytic and photocatalytic removal of methomyl in deionized, distilled and seawater. Semiconducting oxides (TiO_2 and ZnO) and iron catalysts (Fe-ZSM-5 and AlFe-pillared montmorillonite) were used in the photocatalytic reactions. Monochromatic, polychromatic, and natural solar light were applied as light sources during the methomyl removal. The effects of parameters such as water type, reaction temperature, lamp distance, initial concentration of catalyst, initial salt concentration (NaCl), and pH were studied. The effect of various catalysts on the photodegradation of methomyl was also studied.

EXPERIMENTAL

Materials

All chemicals used in this investigation were of reagent grade and were used without further purification. Analytical grade methomyl (99.8%) and technical grade methomyl (98%) were granted by Du Pont De Nemours, USA. TiO_2-Merck Eusolex® T (anatase modification) and ZnO (Merck) were used as received. The preparations of the Fe-ZSM-5 zeolite and AlFe-pillared montmorillonite catalysts were described at previous papers (28,29). One gram of pillared montmorillonite catalyst contained 5 mmol (iron + aluminum) cations; thus, the iron content amounted to *ca.* 14 wt.%. The applied physico-chemical methods for characterization of the catalyst are given elsewhere (29). In the starting Fe-ZSM-5 zeolite, the Si/Al ratio was 12. The extent of iron exchange resulted in a Fe/Al ratio of 0.75. Thus, the iron content was *ca.* 5 wt.%. NaOH, Na_2CO_3, H_2SO_4, HCl, NaCl, and $NaHCO_3$ were purchased from Merck. Hydrogen peroxide solution (30% v/v) in a stable form was provided by Carlo Erba. The acetonitrile used for the HPLC analysis was HPLC grade and was provided by Fluka. Methanesulfonic acid for ion chromatographic analysis was provided by Fluka. All solutions were freshly prepared with Millipore Waters deionized water ($18.2\,\mathrm{M\Omega\,cm^{-1}}$ at 25°C) prior to use.

Photolytic and Photocatalytic Procedures

All solutions were prepared by dissolving methomyl (without a catalyst or with a certain amount of catalyst) in water (deionized, distilled, sea) with additional degasification for 10 min in an ultrasonic water bath. The initial concentration was $16.22\,\mathrm{mg\,L^{-1}}$.

The photolysis of methomyl with monochromatic irradiation at 254 nm was performed using an Osram mercury lamp (2×8 W). The distance between the lamp and the surface of the solution ranged from 20 to 200 mm. The quartz photoreactor (cylindrical shape, volume 20 mL) was equipped with a water-cooled quartz jacket to maintain the solution temperature constant (mainly 20°C) during irradiation. Samples (15.0 mL) were exposed to irradiation from 120 to 600 min. During the experiments, the reaction mixture was stirred on a magnetic stirrer.

Irradiations under UV light (366 nm) were performed in the same quartz photoreactor as mentioned previously with an Osram mercury lamp (2×8 W) placed 50 mm from the surface of the reaction mixture. The experiments under 315–400 nm polychromatic light were performed in a glass reactor (cylindrical shape, volume 30.0 mL) with an 300 W Osram Ultra-Vitalux® lamp (mixture of lights; UV-A:UV-B = 13.6:3, according to the manufacturer's specifications) placed 300 mm from the surface of the reaction mixture. In a typical experiment, 15.0 mL of the methomyl solution for the first or 25.0 mL for the second experiment were used. Agitation was then applied (500 rpm) to maintain a homogenous suspension and the lamp was switched on. After an appropriate irradiation time, the suspension was sampled.

Reactions under sunlight were performed in open flasks made of a quartz glass (150.0 mL volume). In a typical experiment, 100.0 mL of the methomyl solution with a certain amount of TiO_2 or ZnO catalyst were exposed to sunlight for an appropriate time interval (from 20 to 45 h). The average methomyl solution temperature was 35°C.

All solutions of methomyl for the photo-Fenton experiments were prepared by dissolving the analytical grade methomyl in deionized water followed by sonication for 10 min. The reactions were performed at room temperature in a glass batch reactor. A total of 100.0 mL of solution was placed into the reactor together with 2.0 mL $0.1\,\mathrm{mol\,L^{-1}}$ H_2O_2 and a certain amount of Fe-ZSM-5 zeolite or alternatively well-powdered AlFe-pillared clay catalyst. The pH adjustment (3.5–4.0) was realized by adding $0.15\,\mathrm{mol\,L^{-1}}$ H_2SO_4. Solution pH was measured using a PHM 93 reference pH meter, Radiometer, Copenhagen, Denmark. The reaction was performed under vigorous stirring with a constant airflow of $30–35\,\mathrm{mL\,min^{-1}}$. A halogen lamp (Brilux, Model JCDR, 50 W, 640 cd, China) was used as the radiation source. The color temperature of the light was 3000 K, which corresponds to 575.6 nm (30). At the end of the reaction, all solutions were centrifuged for 15 min in a Rotofix 32 centrifuge, Germany, to separate the catalyst particles.

Analytical Procedure

For the spectrophotometric determination methomyl during its degradation of, 2.0 mL of the solution were taken at regular intervals and their spectra recorded (after sample centrifugation when catalysts were used) on a Shimadzu 1700 UV-VIS spectrophotometer in the wavelength range from 200 to 300 nm. The kinetics of methomyl degradation was monitored at 233.8 nm. For HPLC determination, all solutions were filtered through Sartorius 0.20 μm syringe filters and were analyzed at 234 nm and at ambient temperature (25°C) on a Hewlett Packard HP 1050 liquid chromatograph with a UV/VIS detector, equipped with a reversed-phase column type Zorbax Eclipse XDB-C18 150×4.6 mm (i.d.) $\times$ 5 μm. The mobile phase (flow rate $2.0\,\mathrm{mL\,min^{-1}}$) was a mixture of acetonitrile and water (25:75, v/v). The sample injection volume was 20 μL and both samples and standards were diluted with acetonitrile. Under the above chromatographic conditions, the concentrations of methomyl were determined from the peak area at $t_R = 2.0$ min. The sample pH was adjusted by adding dilute NaOH and HCl using a pH meter (PHM93 reference pH meter, Radiometer, Copenhagen, Denmark). For the ion chromatographic determinations, all methomyl solutions were diluted, filtered through Milex-GV 0.22 μm membrane filters, and analyzed on a Dionex DX-300 ion chromatograph at ambient temperature (25°C), with a suppressed conductivity detector. The ion chromatograph was equipped with a Dionex IonPac AS 14 column 250×4.0 mm (i.d.) for anion determination and a Dionex IonPac CS 12 column 250×4.0 mm (i.d.) for cation determination. The mobile phase for the anion determination was a carbonate/bicarbonate mixture ($3.5\,\mathrm{mmol\,L^{-1}}$ Na_2CO_3 + $1.0\,\mathrm{mmol\,L^{-1}}$ $NaHCO_3$), flow rate $1.0\,\mathrm{mL\,min^{-1}}$, and for cation determination, it was a solution of methanesulfonic acid ($20.0\,\mathrm{mmol\,L^{-1}}$), flow rate $1.0\,\mathrm{mL\,min^{-1}}$. The sample injection volumes were 50 μL for both the anion and cation measurements. Prior to sample measurements, blank samples of deionized water were chromatographed. The retention times for nitrate and sulfate ions were 8.0 and 12.5 min, respectively. The retention time for ammonium ions was 4.8 min. For total organic carbon (TOC) analysis, the samples were analyzed on a Zellweger LabTOC 2100 instrument using high-temperature combustion followed by infrared CO_2 detection.

RESULTS AND DISCUSSION

Photolysis

All the experiments were performed under monochromatic 254 nm ultraviolet light since 366 nm ultraviolet light had small effect on methomyl photolysis, as previously established (21).

In the first part of the experimental work, the influence of lamp distance on the reaction rate of methomyl photolysis was studied. The distance between the lamp and the solution surface was varied from 20 to 200 mm. As can be seen from Fig. 2, the reaction rate of methomyl removal decreased with increasing lamp distance. The reaction rate was 3.7 times higher ($k = 0.0194\,\text{min}^{-1}$) when the lamp was placed at 20 mm distance from the reaction mixture surface than when the lamp was placed at 200 mm ($k = 0.0053\,\text{min}^{-1}$). After 120 min irradiation, 29.18% (200 mm), 43.32% (100 mm), 59.89% (50 mm), and 73.62% (20 mm) of the initial technical grade methomyl had been removed at 20°C in distilled water of pH 6.0.

The kinetics of the photodegradation rate of most organic contaminants (31) can be well described using a pseudo-first kinetic order, which is given by the following equations:

$$\ln(C_o/C) = k \cdot t \tag{17}$$

$$C = C_o e^{-k \cdot t} \tag{18}$$

where C_o is the initial concentration of contaminant and C is the concentration of contaminant at irradiation time t, and k is the pseudo-first order rate constant. For reactions of pseudo-first order, the half time of the reaction can be calculated using:

$$t_{1/2} = \ln 2/k \tag{19}$$

All the following experiments using 254 nm radiation were performed with the same Osram mercury lamp (2 × 8 W) placed 100 mm above the surface of the reaction mixture due to the optimal handling of the experiment. The influence of the reaction temperature on the reaction rate of removal of the technical grade methomyl is presented in Fig. 3, which shows that the reaction rate increased in the temperature range from 10°C ($k = 0.0076\,\text{min}^{-1}$) to 50°C ($k = 0.0098\,\text{min}^{-1}$), while the half-lives decreased from 91.20 min to 70.73 min, respectively. It is obvious that the reaction temperature has a significant influence on the degradation reaction rate of the technical grade methomyl in distilled water at pH 6.0. In the further studies, a reaction temperature of 20°C was chosen since the highest increase in the reaction rate was between 10°C and 20°C (the reaction rate constants were $0.0076\,\text{min}^{-1}$ and $0.0087\,\text{min}^{-1}$, respectively).

The influence of the water type was investigated by conducting experiments at 254 nm in deionized (water pH 5.2), distilled (water pH 5.5), and seawater (water pH 7.9, concentration of Cl^- ions, $26.2\,\text{g L}^{-1}$). First, an experiment in the dark at ambient temperature was performed in order to check the stability of methomyl. No methomyl disappearance was detected after seven days. The results of the influence of the type of water are shown in Fig. 4 and Table 1. The reaction rate was highest in distilled water and lowest in seawater. The technical grade methomyl disappeared approximately 1.5 times faster in distilled ($t_{1/2} = 79.67$ min) than in seawater ($t_{1/2} = 123.78$ min) and 1.2 times faster in distilled than in deionized water ($t_{1/2} = 97.63$ min). One would expect the reaction to proceed faster in deionized than in distilled water due to the content of ions in the latter, but the obtained results

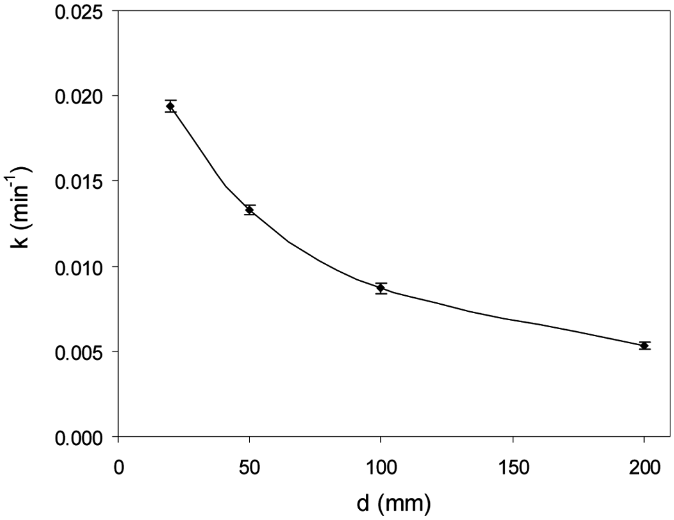

FIG. 2. The effect of lamp distance on the photolysis rate of technical grade methomyl in distilled water ($\lambda = 254$ nm, temperature = 20°C, pH = 6.0).

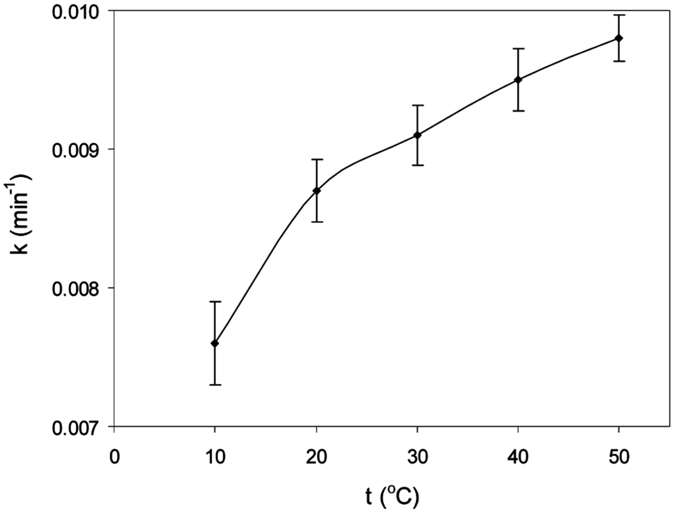

FIG. 3. The effect of temperature on the photolysis rate of technical grade methomyl in distilled water ($\lambda = 254$ nm, lamp distance = 100 mm, pH = 6.0).

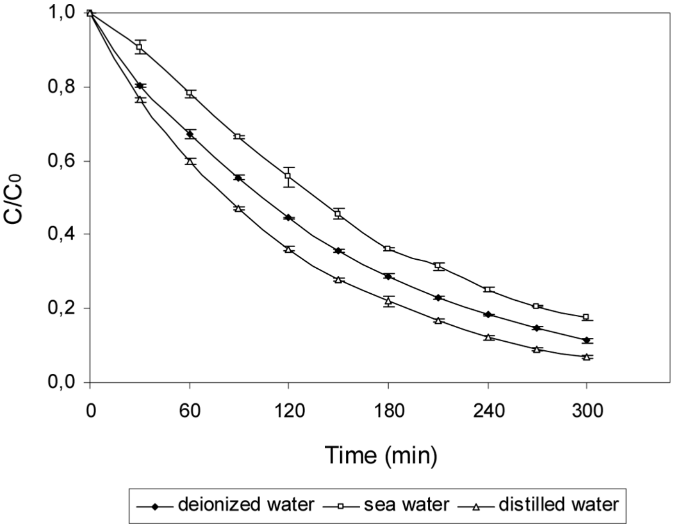

FIG. 4. The effect of the type of water on the photolysis rate of technical grade methomyl ($\lambda = 254$ nm, lamp distance = 100 mm, temperature = 20°C).

suggest that certain ions in distilled water promote the reaction. It is known that distilled water may contain some trace metals as well as trace organic carbon (32). In addition, it was found that Cu^{2+} in combination with ascorbic acid promotes the removal of bisphenol A in aqueous solution (33). Seawater contains different ions, such as Cl^-, SO_4^{2-}, HCO_3^-, etc. (20) which can retard the photolysis of methomyl. It was found that the reactions in the different waters followed first-order kinetics, as given in Table 1.

In general, photolysis of chemicals in aqueous solution is influenced by pH. In the present study two experiments were performed using 254 nm irradiation. First, the photolysis of the technical grade methomyl was studied in distilled water at three different pH values (3.15, 6.00, and 10.55). The pH was adjusted by the addition of HCl (3.15) or NaOH (10.55). The third value is the pH of the pure insecticide solution in distilled water. The obtained results (Fig. 5 and Table 2) imply that the pH has small influence on the reaction rate and that the reaction was the fastest at pH = 6.0. Removal of the analytical grade methomyl was studied in deionized water at five different

TABLE 1
Kinetics of methomyl degradation under artificial lights and sunlight

			Water type		
Light source	Technical methomyl	Parameters	Deionized	Distilled	Sea
254 nm	Without a catalyst	k (min^{-1})	0.0071	0.0087	0.0056
		R	0.9990	0.9991	0.9942
		$t_{1/2}$ (min)	97.63	79.67	123.78
366 nm	With 2.0 g L^{-1} of TiO_2	k (min^{-1})	0.0058		
		R	0.9880		
		$t_{1/2}$ (min)	119.51		
	With 2.0 g L^{-1} of ZnO	k (min^{-1})	0.0120		
		R	0.9915		
		$t_{1/2}$ (min)	57.76		
315–400 nm	With 2.0 g L^{-1} of TiO_2	k (min^{-1})	0.0047		
		R	0.9941		
		$t_{1/2}$ (min)	147.48		
	With 2.0 g L^{-1} of ZnO	k (min^{-1})	0.0100		
		R	0.9988		
		$t_{1/2}$ (min)	69.31		
Sunlight	With 0.1 g L^{-1} of TiO_2	k (min^{-1})	0.0018	0.0030	0.00046
		R	0.9976	0.9985	0.9930
		$t_{1/2}$ (min)	387.59	228.38	1501.42
	With 0.2 g L^{-1} of TiO_2	k (min^{-1})	0.0016	0.0022	0.00057
		R	0.9955	0.9993	0.9803
		$t_{1/2}$ (min)	443.85	320.41	1208.98
	With 0.15 g L^{-1} of ZnO	k (min^{-1})	0.0019	0.0028	0.00114
		R	0.9989	0.9975	0.9945
		$t_{1/2}$ (min)	364.81	250.53	605.37

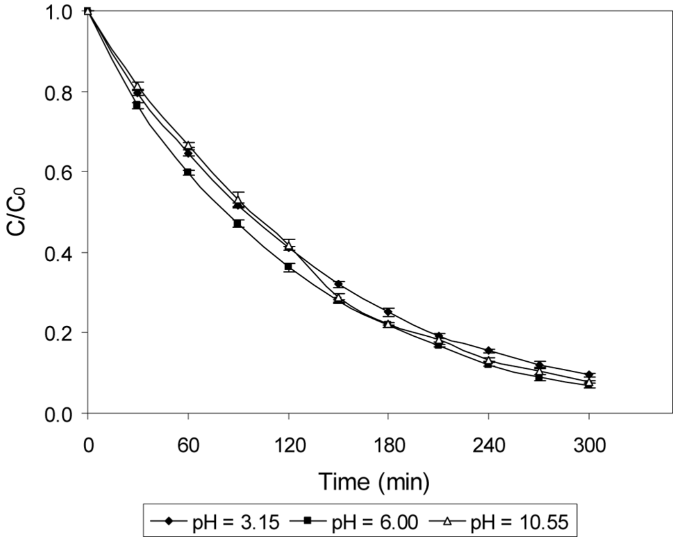

FIG. 5. The effect of pH on the photolysis rate of technical grade methomyl in distilled water ($\lambda = 254$ nm, lamp distance = 100 mm, temperature = 20°C).

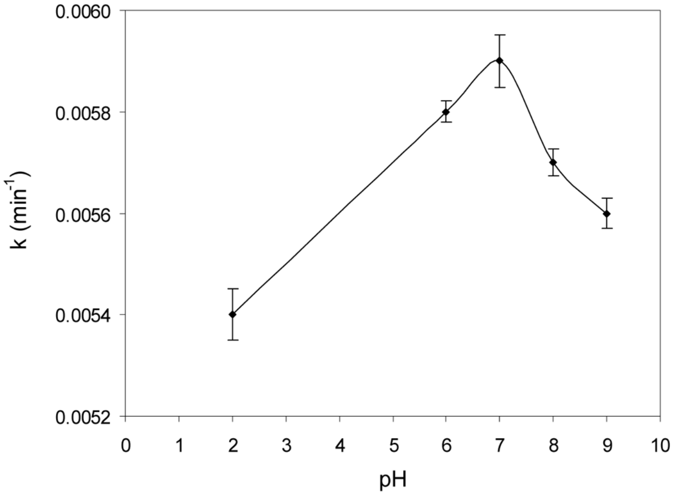

FIG. 6. The effect of pH on the photolysis rate of analytical grade methomyl in deionized water ($\lambda = 254$ nm, lamp distance = 100 mm, temperature = 20°C).

pH values (2.0, 6.0, 7.0, 8.0, and 9.0). The obtained results are shown in Fig. 6 and Table 2. Once again, it can be seen that the reaction rate was the highest in neutral and the lowest in acidic media. In addition, it is obvious from Table 2 that at pH = 6.0 in deionized water, the technical grade methomyl disappeared faster ($k = 0.0071\,\text{min}^{-1}$) than the analytical grade methomyl ($k = 0.0058\,\text{min}^{-1}$), but slower than the technical grade methomyl in distilled water ($k = 0.0087\,\text{min}^{-1}$).

Photocatalytic Removal of Methomyl Under 366 nm and 315–400 nm Radiation

The influence of various parameters, such as the initial concentration of the catalyst, the initial NaCl concentration and pH, was investigated on the photocatalytic removal of methomyl in the presence of TiO_2 and ZnO using an Osram mercury or a 300 W Osram lamp. The effect of various catalysts on the methomyl photocatalytic removal was also studied. In the first part of the photocatalytic study, several experiments were conducted in deionized water under 366 nm and 315–400 nm light. These experiments were performed using different conditions, i.e., in the absence and presence of the catalyst as well as in the dark. In the absence of the catalyst, no changes in methomyl concentration were observed under either monochromatic or polychromatic light. In the absence of light, a very small change in the methomyl concentration was observed. In the third experiment, when either type of radiation and TiO_2 or ZnO were applied, a disappearance of methomyl was registered (Table 1).

TABLE 2
Effect of pH on the kinetics of methomyl degradation under 254 nm irradiation (temperature: 20°C, lamp distance: 100 mm)

			pH						
Water type	Methomyl	Parameters	2.00	3.15	6.00	7.00	8.00	9.00	10.15
Distilled	Technical	k (min^{-1})		0.0078	0.0087				0.0083
		R		0.9993	0.9991				0.9970
		$t_{1/2}$ (min)		88.86	79.67				83.51
Deionized	Analytical	k (min^{-1})	0.0054		0.0058	0.0059	0.0057	0.0056	
		R	0.9977		0.9983	0.9993	0.9964	0.9956	
		$t_{1/2}$ (min)	128.36		119.51	117.48	121.61	123.78	
Deionized	Technical	k (min^{-1})			0.0071				
		R			0.9990				
		$t_{1/2}$ (min)			97.63				

The most employed semiconductor photocatalyst TiO_2, as well as ZnO were used. The most important advantage of ZnO over TiO_2 is that it absorbs over a larger range of the UV spectrum. All experiments were performed using $1.0-3.0\,g\,L^{-1}$ of either TiO_2 or ZnO and it was found that the optimal concentration of the catalysts was $2.0\,g\,L^{-1}$. The photodegradation efficiency increased with increasing concentration of the photocatalyst, reaching the highest value at $2.0\,g\,L^{-1}$ and then decreasing. A possible explanation for this phenomenon is that when all insecticide molecules are adsorbed by TiO_2, the addition of higher quantities of TiO_2 has no effect on the photodegradation efficiency but the increased catalyst concentration in the solution causes light inhibition due to the opacity it creates. For this reason, reduced degradation rates were registered when the catalyst concentration was increased beyond $2.0\,g\,L^{-1}$. In addition, the results (Fig. 7 and Table 1) showed that the photocatalytic removal of methomyl was much faster when ZnO was used ($k = 0.0120\,min^{-1}$ for the 366 nm lamp and $k = 0.0100\,min^{-1}$ for the 300 W Osram lamp) than when TiO_2 was used ($k = 0.0058\,min^{-1}$ for the 366 nm lamp and $k = 0.0047\,min^{-1}$ for the 300 W Osram lamp). As a result, the methomyl disappeared approximately 1.2 times faster under 366 nm than under 315–400 nm light. The methomyl removal rate in the presence of ZnO was approximately twice that registered in the presence of TiO_2 (catalyst concentration $= 2.0\,g\,L^{-1}$).

It is also known that the degradation of some organic compounds in photocatalytic processes is influenced by the pH value of the solution (34,35). The photocatalytic removal of methomyl was studied at three different pH values (3.5, 5.6, and 9.0), adjusted by the addition of HCl (3.5) or NaOH (9.0), while the third pH value was that of the pure insecticide solution in deionized water. The results imply that the removal rate was the highest in acidic solution and the lowest in alkaline solution. It should be mentioned that the pH of the solution can also be adjusted by the addition of H_2SO_4 or HF. The addition of either HF or H_2SO_4 practically doubled the degradation rate of 2-hydroxypyridine when P-25 was used, as reported by Stapleton et al. (36). This can be explained by the adsorption of free fluoride ions on the surface of the catalyst and the displacement of surface bound hydroxyl radicals (37–40). Also, SO_4^{2-} ions could be adsorbed onto the catalyst surface, thus modifying surface properties (acidity, area, electron–hole recombination) (41,42).

A common inorganic salt, i.e., sodium chloride, was applied to study the influence of an inorganic salt on the photocatalytic removal of methomyl. The influence of different concentrations of sodium chloride (0.0–5.0% w/v) on the reaction rate is presented in Fig. 8. The observed decrease of the reaction rate of methomyl removal in the presence of chloride ions can be explained by competitive adsorption or by the hole scavenging properties of chloride ions (43):

$$Cl^- + h^+_{VB} \rightarrow Cl^{\cdot} \tag{20}$$

$$Cl^{\cdot} + Cl^- \rightarrow Cl_2^{-\cdot} \tag{21}$$

$$OH^{\cdot} + Cl^- \rightarrow Cl^{\cdot} + OH^- \tag{22}$$

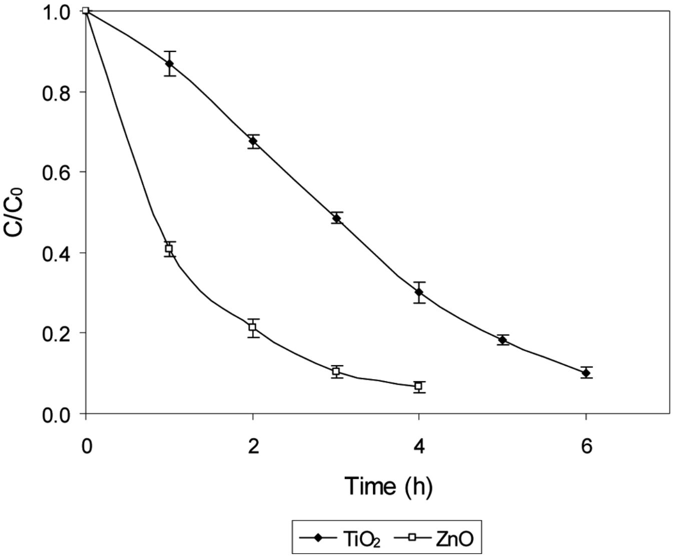

FIG. 7. The effect of the catalyst type on the photocatalytic removal rate of methomyl in deionized water ($\lambda = 366\,nm$, pH = 5.6, catalyst concentration $= 2.0\,g\,L^{-1}$).

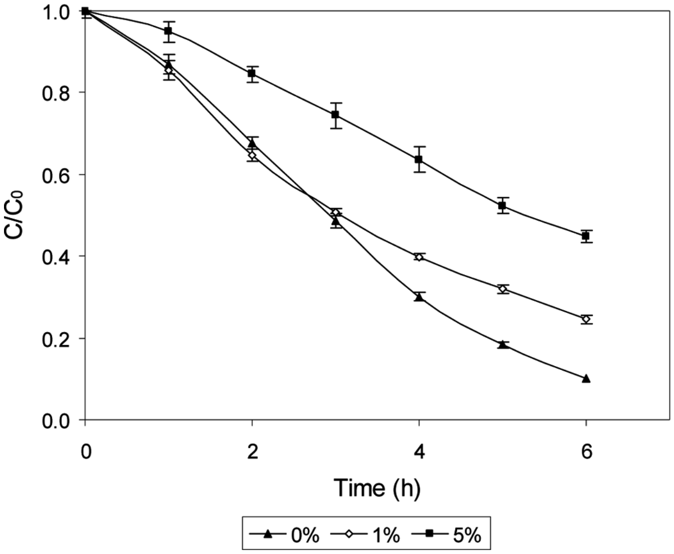

FIG. 8. The effect of the NaCl concentration on the photocatalytic removal rate of methomyl in deionized water ($\lambda = 366\,nm$, pH = 5.6, $TiO_2 = 2.0\,g\,L^{-1}$).

While chlorine radicals are formed slowly, they are converted into chloride anions instantly. The surface sites normally available at the TiO_2/methomyl solution interface for adsorption and electron transfer from methomyl can be blocked by anions, such as chloride anions, which are not oxidizable and are effective inhibitors of the detoxification process (43).

The ion chromatography results showed that mineralization led to the formation of sulfate, nitrate, and ammonium ions during the process, both under monochromatic and polychromatic light (Figs. 9 and 10). Mineralization of sulfur atoms into sulfate ions was almost complete and the maximum expected value for sulfate ions (around $9.60\,mg\,L^{-1}$) was obtained. Nitrate and ammonium ions were also detected in various relative concentrations during the photocatalytic experiments. The maximum detected value for nitrate and ammonium ions were $1.13\,mg\,L^{-1}$ and $1.22\,mg\,L^{-1}$, respectively. The nitrogen mass balance was therefore incomplete at the end of the treatment (around 50% of the inorganic nitrogen expected in the process). When TiO_2 was used as the catalyst, mineralization of organic carbon was incomplete and about 80% of the initial TOC had disappeared after 8 h (under 300 W Osram lamp) or after 6 h (under 366 nm). These results are in accordance with those of other researchers (24). In addition, it was found that ZnO was a better catalyst than TiO_2. When ZnO was used about 80% of the initial TOC had disappeared after 4 h (Figs. 9 and 10).

Sunlight Degradation of Methomyl

AOPs driven by solar energy appears to be an efficient method for the removal of pesticides from water (16, 24–26). The influence of the initial concentration of catalysts and effects of various catalysts on methomyl removal in deionized, distilled, and seawater was investigated. All experiments were performed with $0.1\,g\,L^{-1}$ or $0.2\,g\,L^{-1}$ of TiO_2 and with $0.15\,g\,L^{-1}$ of ZnO. Several experiments were performed prior to the photocatalysis tests with TiO_2 and ZnO. The experiments in which $16.22\,mg\,L^{-1}$ methomyl solutions in the absence of catalyst (in the three water type) were exposed to sunlight for five days showed no changes in the methomyl concentration. Also, experiments in the dark with both the TiO_2 and ZnO catalyst confirmed that no alterations were detected in solutions containing initially $16.22\,mg\,L^{-1}$ of methomyl. Subsequently, methomyl solutions with both catalysts, either TiO_2 or ZnO, were exposed to sunlight from 20 to 45 h, depending on the kind of water which was used as the solvent.

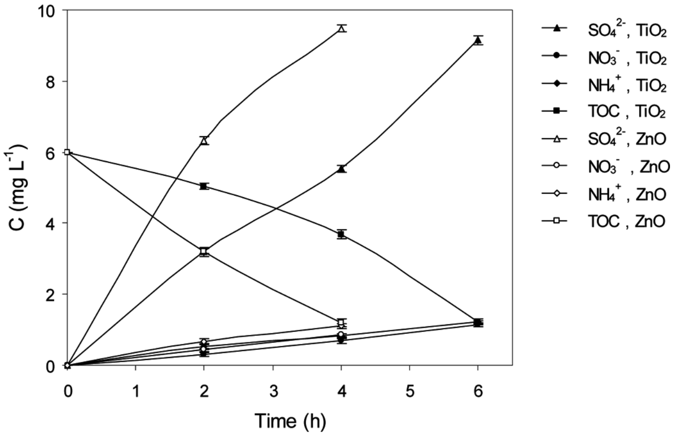

FIG. 9. Disappearance and mineralization of methomyl under 366 nm UV light (deionized water, pH = 5.6, catalyst concentration = $2.0\,g\,L^{-1}$).

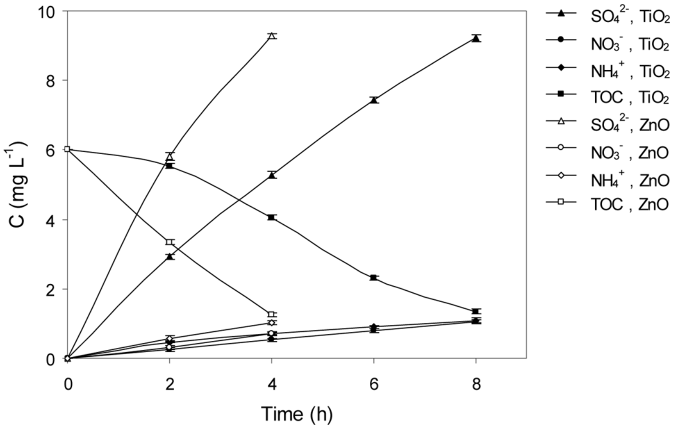

FIG. 10. Disappearance and mineralization of methomyl under the 300 W Osram Ultra-vitalux lamp ($\lambda = 315$–$400\,nm$, deionized water, pH = 5.6, catalyst concentration = $2.0\,g\,L^{-1}$).

The results of the photocatalytic removal methomyl under sunlight are presented in Table 1. In all cases the dissipation of methomyl followed a pseudo-first kinetic order. When $0.1\,g\,L^{-1}$ of TiO_2 was used, the rate constant of methomyl removal from distilled water ($k = 0.0030\,min^{-1}$) was 1.7 or 6.5 times faster than that in deionized ($k = 0.0018\,min^{-1}$) or seawater ($k = 0.00045\,min^{-1}$). In the presence of $0.2\,g\,L^{-1}$ of TiO_2, the methomyl disappeared 1.4 times faster in distilled ($t_{1/2} = 320.41$ min) than in deionized water ($t_{1/2} = 443.85$ min) and 3.9 times faster than in seawater ($t_{1/2} = 1208.98$ min). The disappearance of methomyl was 1.5 times faster in the presence of $0.15\,g\,L^{-1}$ of ZnO as a catalyst in distilled water ($k = 0.0028\,min^{-1}$) than in deionized water ($k = 0.0019\,min^{-1}$) and 2.5 times faster than in seawater ($k = 0.00114\,min^{-1}$). As can be seen from Table 1, ZnO was generally a better catalyst than TiO_2. In seawater, methomyl was degraded approximately 2 times faster in the presence of ZnO than in the presence of TiO_2.

IC analysis confirmed that when deionized or distilled water were used as solvents, the all the sulfur present in the methomyl molecule was released as sulfate anions, which is in agreement with the results presented in other reports (23–25). Ammonium and nitrate anions were also detected in various relative concentrations during the photocatalytic experiments in deionized and distilled water, as was reported elsewhere (24). The amount of ammonium anions detected during sunlight removal of methomyl was higher and the amount of nitrate anions was lower than under the artificial lights.

Methomyl Removal Under Photo-Fenton Process

In the experimental work focusing on catalytic wet peroxide oxidation of methomyl at 575.6 nm (photo-Fenton reaction), two types of heterogeneous iron catalysts were used: Fe-ZSM-5 zeolite at a concentration of $1\,g\,L^{-1}$ and AlFe-pillared montmorillonite at a concentration of $5\,g\,L^{-1}$. The effect of catalyst concentration on the reaction is shown in Fig. 11. When the AlFe-pillared clay catalyst was used, only 54% of the methomyl had been degraded after 5 h of illumination, while methomyl conversion with Fe-ZSM-5 zeolite exceeded 80% after 1 h of reaction and almost 100% of the methomyl had been degraded after 4 h of irradiation. It is obvious that the activity of the Fe-ZSM-5 zeolite was significantly higher as compared to the AlFe-pillared clay catalyst. Another problem with the AlFe-pillared clay catalyst was that the intermediates of the product retarded the functioning of the catalyst. The absorbance of the methomyl solution after 4 and 5 h reaction time were practically the same (Fig. 11). This retardation phenomenon was similar to the phenomenon observed in phenol degradation (28). A further advantage of the Fe-ZSM-5 over AlFe-pillared clay catalyst is its easier separation from the reaction suspension. The Fe-ZSM-5 catalyst precipitates easily on the bottom of the glass reactor, while removal of the AlFe- pillared clay catalyst from the reaction suspension can proceed, with reasonable velocity, only by centrifugation (27). In addition, comparing the two catalysts, it is evident that the structure of the zeolite certainly stabilizes iron in a state favorable for the catalytic process (44). Ion chromatography results showed that mineralization led to sulfate, nitrate and ammonium ions during the process.

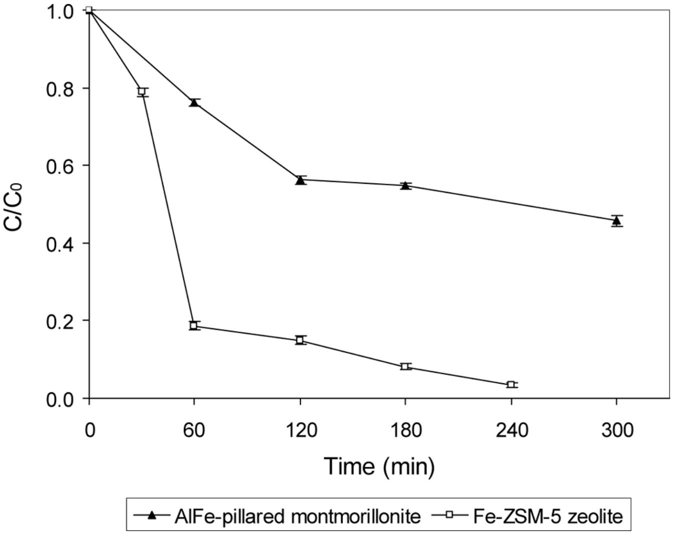

FIG. 11. Methomyl disappearance under the photo-Fenton process ($\lambda = 575.6$ nm, deionized water, catalyst concentration: Fe-ZSM-5 zeolite $= 1\,g\,L^{-1}$, AlFe-pillared montmorillonite $= 5\,g\,L^{-1}$).

CONCLUSIONS

For the first time, it is reported that methomyl can be effectively decomposed by ultraviolet light at 254 nm in various aqueous solutions, including seawater. The reaction rate depends on the water type, lamp distance, reaction temperature, and pH. The reaction rate of methomyl removal decreased with increasing lamp distance and was the lowest in seawater. In addition, it was found that the reaction rate increases in the temperature range from 10°C to 50°C and it is the highest in neutral and the lowest in acidic media. It was previously reported that methomyl can be decomposed by UV light λ_{max} at 366 nm (21–23) and sunlight (16,24–26) using Degussa P-25 TiO_2, UV light λ_{max} at 366 nm (23) using ZnO (Merck) and TiO_2 Hombikat UV-100. The present results of the photocatalytic removal of methomyl by UV light (366 nm) and by simulated solar light (315–400 nm) indicated that the reaction was affected by the initial catalyst concentration, pH and the type of catalyst, as reported previously (21). It was found earlier that P-25 TiO_2 is a better catalyst than ZnO (Merck) and TiO_2 Hombikat UV-100 (anatase) (23). In the present study, it was also found that ZnO (Merck) is a better catalyst than TiO_2 (Merck) (anatase) under the same reaction conditions. It was also found that the presence of NaCl led to an inhibition of the reaction due to the scavenging properties of chloride ions, as reported earlier (21). Concerning the photo-Fenton reaction, it was reported by Tamimi et al. (14) that methomyl can be removed by photo-Fenton ($H_2O_2/Fe^{2+}/UV$) in 30 min. Here and in a previous paper (27), it was demonstrated that Fe-ZSM-5 zeolite and AlFe-pillared montmorillonite show significant activity in the photo-Fenton reaction, the Fe-ZSM-5 zeolite being the superior catalyst. In both the photocatalytic and photo-Fenton reaction, IC results showed that mineralization led to the formation of sulfate, nitrate, and ammonium ions during the processes, while Tamimi et al. (22) reported the formation of only sulfate and ammonium ions.

ACKNOWLEDGEMENTS

The authors are grateful to the Ministry of Science and Technological Development of the Republic of Serbia for financial support (Projects TR 20041 and 142063). Also, the authors acknowledge the financial support provided by the European Agency for Reconstruction through the Ministry of International Economic Relations within the

Neighboring Program Hungary-Serbia (Action entitled "Regional Water Resources Investigations in the Scope of Sustainable Development", Grant No. 04SER02/01/009). They also wish to thank Mr Aleksandar F. Tomaši for technical assistance.

REFERENCES

1. Tomlin, C.D.S. (ed.) (2006) *The Pesticide Manual*, 14th Ed.; BCPC: Oxford, U.K.
2. Hassall, K.A. (1990) *The Biochemistry and Uses of Pesticides*, 2nd Ed.; VCH: New York, U.S.A.
3. Strathmann, T.J.; Stone, A.T. (2001) Reduction of the carbamate pesticides oxamil and methomyl by dissolved Fe^{II} and Cu^{I}. *Environ. Sci. Technol.*, 35: 2461–2469.
4. Legrini, O.; Oliveros, E.; Braun, A.M. (1993) Photochemical processes for water treatment. *Chem. Rev.*, 93: 671–698.
5. Sun, Y.; Pignatello, J.J. (1993) Photochemical reactions involved in the total mineralization of 2,4-D by $Fe^{3+}/H_2O_2/UV$. *Environ. Sci. Technol.*, 27: 304–310.
6. Andreozzi, R.; Caprio, V.; Insola, A.; Marotta, R. (1999) Advanced oxidation processes (AOP) for water purification and recovery. *Catal. Today*, 53: 51–59.
7. Neyens, E.; Baeyens, J. (2003) A review of classic Fenton's peroxidation as an advanced oxidation technique. *J. Hazard. Mat. B*, 98: 33–50.
8. Gomes da Silva, C.; Faria, J.L. (2003) Photochemical and photocatalytic degradation of an azo dye in aqueous solution by UV irradiation. *J. Photochem. Photobiol. A: Chem.*, 155: 133–143.
9. Daneshvar, N.; Salari, D.; Khataee, A.R. (2003) Photocatalytic degradation of azo dye Acid Red 14 in water: Investigation of the effect of operational parameters. *J. Photochem. Photobiol. A: Chem.*, 157: 111–116.
10. Karkmaz, M.; Puzenat, E.; Guillarad, C.; Herrmann, J.M. (2004) Photocatalytic degradation of the alimentary azo dye Amaranth. Mineralization of the azo group to nitrogen. *Appl. Catal. B: Environ.*, 51: 183–194.
11. Daneshvar, N.; Salari, D.; Khataee, A.R. (2004) Photocatalytic degradation of azo dye acid red 14 in water on ZnO as an alternative catalyst to TiO_2. *J. Photochem. Photobiol. A: Chem.*, 162: 317–322.
12. Behnajady, M.A.; Modirshahla, N.; Hamzavi, R. (2006) Kinetic study on photocatalytic degradation of C.I. Acid Yellow 23 by ZnO photocatalyst. *J. Hazard. Mater. B*, 133: 226–232.
13. Pera-Titus, M.; Garcia-Molina, V.; Banos, M.A.; Gimenez, J.; Esplugas, S. (2004) Degradation of chlorophenols by means of advanced oxidation processes: a general review. *Appl. Catal. B: Environ.*, 47: 219–256.
14. Tamimi, M.; Qourzal, S.; Barka, N.; Assabbane, A.; Ait-Ichou, Y. (2008) Methomyl degradation in aqueous solutions by Fenton's reagent and the photo-Fenton system. *Sep. Purif. Technol.*, 61: 103–108.
15. Feng, W.; Nansheng, D. (2000) Photochemistry of hydrolytic iron(III) species and photoinduced degradation of organic compounds. A mini review. *Chemosphere*, 41: 1137–1147.
16. Malato, S.; Blanco, J.; Cáceres, J.; Fernandez-Alba, A.R.; Agüera, A.; Rodriguez, A. (2002) Photocatalytic treatment of water-soluble pesticides by photo-Fenton and TiO_2 using solar energy. *Catal. Today*, 76: 209–220.
17. Malato, S.; Blanco, J.; Vidal, A.; Richter, C. (2002) Photocatalysis with solar energy at a pilot-plant scale: an overview. *Appl. Catal. B: Environ.*, 37: 1–15.
18. Liu, S.; Li, Q.X. (2004) Photolysis of spinosins in seawater, stream water and various aqueous solutions. *Chemosphere*, 56: 1121–1127.
19. Campbell, S.; David, M.D.; Woodward, L.A.; Li, Q.X. (2004) Persistence of carbofuran in marine sand and water. *Chemosphere*, 54: 1155–1161.
20. Navarro, S.; Vela, N.; Gimenez, M.J.; Navarro, G. (2004) Persistence of four *s*-triazine herbicides in river, sea and groundwater samples exposed to sunlight and darkness under laboratory conditions. *Sci. Total Environ.*, 329: 87–97.
21. Tamimi, M.; Belmouden, M.; Qourzal, S.; Assabbane, A.; Ait-Ichou, Y. (2006) Photocatalytic degradation of methomyl with the presence of titanium dioxide (Degussa P-25). *Fres. Environ. Bullet.*, 15: 1226–1231.
22. Tamimi, M.; Qourzal, S.; Assabbane, A.; Chovelon, J.M.; Ferronato, C.; Ait-Ichou, Y. (2006) Photocatalytic degradation of pesticide methomyl: Determination of the reaction pathway and identification of intermediate products. *Photochem. Photobiol. Sci.*, 5: 477–482.
23. Poulios, I.; Kositzi, M.; Pitarakis, K.; Beltsios, S.; Oikonomou, I. (2006) Photocatalytic oxidation of methomyl in the presence of semiconducting oxides. *Int. J. Environ. Pollut.*, 28: 33–44.
24. Oller, I.; Gernjak, W.; Maldonado, M.I.; Pérez-Estrada, L.A.; Sánchez-Pérez, J.A.; Malato, S. (2006) Solar photocatalytic degradation of some hazardous water-soluble pesticides at pilot-plant scale. *J. Hazard. Mater. B*, 138: 507–517.
25. Fernández-Alba, A.R.; Hernando, D.; Agüera, A.; Cáceres, J.; Malato, S. (2002) Toxicity assays: a way for evaluating AOPs efficiency. *Water Res.*, 36: 4255–4262.
26. Malato, S.; Blanco, J.; Vidal, J.; Alacrón, D.; Maldonado, M.I.; Cáceres, J.; Gernjak, W. (2003) Applied studies in solar photocatalytic detoxification: An overview. *Sol. Energy*, 75: 329–336.
27. Tomašević, A.; Bošković, G.; Mijin, D.; Kiss, E.E. (2007) Decomposition of methomyl over supported iron catalysts. *React. Kinet. Catal. Lett.*, 91: 53–59.
28. Kiss, E.E.; Ranogajec, J.G.; Marinković-Nedučin, R.P.; Vulic, T.J. (2003) Catalytic wet peroxide-oxidation of phenol over AlFe-pillared montmorillonite. *React. Kinet. Catal. Lett.*, 80: 255–260.
29. Kiss, E.E.; Lazic, M.M.; Boskovic, G.C. (2004) AlFe-pillared clay catalyst for phenol oxidation in aqueous solution. *React. Kinet. Catal. Lett.*, 83: 221–227.
30. Borbely, A.; Samson, A.; Schanda, J. (2001) The concept of correlated colour temperature revisited. *Color Res. Appl.*, 26: 450–457.
31. Konstantinou, I.K.; Albanis, T.A. (2003) Photocatalytic transformation of pesticides in aqueous titanium dioxide suspensions using artificial and solar light: Intermediates and degradation pathways. *Appl. Catal. B: Environ.*, 42: 319–335.
32. Csuros, M. (1994) *Environmental Sampling and Analysis for Technicians*; CRC Press: Boca Raton, FL.
33. Peng, Z.; Zhang, X.; Yang, L.; Wu, F.; Deng, N. (2008) Photodegradation of bisphenol A induced by metal ions in aqueous solution in the presence of ascorbic acid. *Wuhan Univ. J. Natur. Sci.*, 13: 107–112.
34. Gupta, H.; Tanaka, S. (1995) Photocatalytic mineralization of perchloroethylene using titanium dioxide. *Water Sci. Technol.*, 31: 47.
35. Wu, C.; Liu, X.; Wei, D.; Fan, J. (2001) Photosonochemical degradation of phenol in water. *Water Res.*, 35: 3927–3933.
36. Stapleton, D.R.; Konstantinou, I.K.; Mantzavinos, D.; Hela, D.; Papadaki, M. (2010). On the kinetics and mechanisms of photolytic/TiO2-photocatalytic degradation of substituted pyridines in aqueous solutions. *Appl. Catal. B: Environ.*, 95: 100–109.
37. Calza, P.; Pelizzetti, E. (2001) Photocatalytic transformation of organic compounds in the presence of inorganic ions. *Pure Appl. Chem.*, 73: 1839–1848.
38. Minero, C.; Mariella, G.; Maurino, V.; Pelizzetti, E. (2000) Photocatalytic transformation of organic compounds in the presence of inorganic anions. 1. Hydroxyl-mediated and direct electron-transfer reactions of phenol on a titanium dioxide-fluoride system. *Langmuir*, 16: 2632–2641.
39. Minero, C.; Mariella, G.; Maurino, V.; Pelizzetti, E. (2000) Photocatalytic transformation of organic compounds in the presence of

inorganic ions. 2. Competitive reactions of phenol and alcohols on a titanium dioxide-fluoride system. *Langmuir*, 16: 8964–8972.

40. Oh, Y.C.; Jenks, W. (2004) Photocatalytic degradation of cyanuric acid, a recalcitrant species. *J. Photochem. Photobiol. A*, 162: 323–328.
41. Wang, Z.-C.; Shui, H.-F. (2007) Effect of PO_4^{3-} and $PO_4^{3-}-SO_4^{2-}$ modification of TiO_2 on its photocatalytic properties. *J. Mol. Catal. A: Chem.*, 263: 20–25.
42. Kozlov, V.; Vorontsov, A.V. (2008) Sulphuric acid and Pt treatment of the photocatalytically active titanium dioxide. *J. Catal.*, 258: 87–94.
43. Neppolian, B.; Choi, H.C.; Sakthivel, S.; Arabindoo, B.; Murugesan, V. (2002) Solar light induced and TiO_2 assisted degradation of textile dye Reactive Blue 4. *Chemosphere*, 46: 1173–1181.
44. Lázár, K.; Tomašević, A.; Bošković, G.; Kiss, E. (2009) Comparison of FeAl-PILC and Fe-ZSM-5 catalysts used for degradation of methomyl. *Hyperfine Interact.*, 192: 23–29.